Positron emission tomography imaging of tau pathology in progressive supranuclear palsy

Sarah Coakeley[1,2], Sang Soo Cho[1,2], Yuko Koshimori[1,2],
Pablo Rusjan[1], Madeleine Harris[1], Christine Ghadery[1,2],
Jinhee Kim[1,2], Anthony E Lang[3], Alan Wilson[1], Sylvain Houle[1]
and Antonio P Strafella[1,2,3]

Abstract
Progressive supranuclear palsy is a rare form of atypical Parkinsonism that differs neuropathologically from other parkinsonian disorders. While many parkinsonian disorders such as Parkinson's disease, Lewy body dementia, and multiple system atrophy are classified as synucleinopathies, progressive supranuclear palsy is coined a tauopathy due to the aggregation of pathological tau in the brain. [^{18}F]AV-1451 (also known as [^{18}F]-T807) is a positron emission tomography radiotracer that binds to paired helical filaments of tau in Alzheimer's disease. We investigated whether [^{18}F]AV-1451 could be used as biomarker for the diagnosis and disease progression monitoring in progressive supranuclear palsy. Six progressive supranuclear palsy, six Parkinson's disease, and 10 age-matched healthy controls were recruited. An anatomical MRI and a 90-min PET scan, using [^{18}F]AV-1451, were acquired from all participants. The standardized uptake value ratio from 60 to 90 min post-injection was calculated in each region of interest, using the cerebellar cortex as a reference region. No significant differences in standardized uptake value ratios were detected in our progressive supranuclear palsy group compared to the two control groups. [^{18}F]AV-1451 may bind selectivity to the paired helical filaments in Alzheimer's disease, which differ from the straight conformation of tau filaments in progressive supranuclear palsy.

Introduction

Progressive supranuclear palsy (PSP) is the most common atypical parkinsonian disorder, with a prevalence of approximately five to six individuals per 100,000.[1,2] This neurodegenerative movement disorder is categorized clinically by postural instability, often leading to unexplained falls, supranuclear gaze palsy, and gait difficulty.[3,4] It is not uncommon for cognitive abilities to decline throughout the course of the disease.[3,5] PSP can be challenging to diagnose clinically. Several clinical subtypes are recognized which overlap with other neurodegenerative disorders such as Parkinson's disease (PD), frontotemporal dementia, and corticobasal degeneration (CBD). There are currently no diagnostic procedures available for a

[1]Research Imaging Centre, Campbell Family Mental Health Research Institute, Centre for Addiction and Mental Health, University of Toronto, Toronto, ON, Canada
[2]Division of Brain, Imaging and Behaviour – Systems Neuroscience, Krembil Research Institute, UHN, University of Toronto, Toronto, ON, Canada
[3]Morton and Gloria Shulman Movement Disorder Unit & E.J. Safra Program in Parkinson Disease, Neurology Division, Department of Medicine, Toronto Western Hospital, UHN, University of Toronto, Toronto, ON, Canada

Corresponding author:
Antonio P Strafella, Toronto Western Hospital and Institute CAMH-Research Imaging Centre, University of Toronto, Toronto, ON, Canada M5T 2S8.
Email: antonio.strafella@camh.ca

definitive diagnosis of this disorder. The most common misdiagnosis of PSP is PD.[6] While many parkinsonian cases can present with common signs, especially in the early stages of the disorders, they differ neuropathologically. PD is classified as a synucleinopathy due to the pathological accumulation of α-synuclein, while PSP is marked by inclusions of the microtubule-associated protein tau and is thereby categorized as a primary tauopathy.[7,8]

Tau is primarily found in neurons under normal conditions.[9] It aids in the assembly and stabilization of microtubules.[9,10] Tau exists in six isoforms; specifically, alternative splicing of exon 10 on tau mRNA yields three repeat (3R) and four repeat (4R) microtubule-binding domains on the C-terminus.[11,12] Localization of tau in the neuron is largely dependent on post-translational modifications of the protein, most notably phosphorylation. Phosphorylated tau is generally found in the soma of the neuron, while unphosphorylated tau is primarily found in the axon. Phosphorylation of tau reduces its affinity for microtubules and also reduces its susceptibility to proteolysis.[12,13] Hyperphosphorylation of tau can cause it to self-aggregate, and a high concentration of hyperphosphorylated tau is found in neurodegenerative disorders.[13,14] Tau can aggregate in neurons to form neurofibrillary tangles (NFT). Glial tau inclusions are found mainly in astrocytes and oligodendrocytes. Differences in tau conformation and distribution generate a variety of tauopathies including PSP, Alzheimer's disease (AD), and CBD. AD is marked by paired helical filaments (PHF) of tau with an approximately equal 3R to 4R ratio,[10,11,15] while in PSP and CBD tau aggregation forms straight filaments of tau, which are primarily composed the 4R isoform.[2,8,10,16] In order to bind pathological tau in all tauopathies, a ligand must have affinity for both conformations and isoforms.

Positron emission tomography (PET) is an imaging modality that can be used to detect biomarkers in vivo. Many PET radiotracers have been recently developed to image tau, such as [18F]FDDNP, [18F]THK-5105, [18F]THK-5117, [18F]THK-5351, and [11C]PBB3.[17–21] [18F]AV-1451, also known as [18F]T807, has shown high selectivity and specificity for PHF tau over β-amyloid in AD brain slices.[22–24] In a preliminary study with AD and mild cognitively impaired individuals (MCI), [18F]AV-1451 was able to significantly distinguish between AD and MCI and healthy controls.[25] A subsequent study was performed with AD, MCI, older controls, and younger controls.[26] The majority of individuals in this study, regardless of diagnosis could be classified by the Braak staging of AD in regards to their [18F]AV-1451 uptake. Older adults tended to have higher [18F]AV-1451 retention when compared to younger adults, though this difference was not statistically significant. These findings were consistent with literature suggesting increased NFT deposition with age.[26]

Currently, there are no validated PET radiotracers available to image tau in PSP patients in a clinical setting. Due to the aggressive nature of PSP, individuals with this disorder could benefit from the diagnostic and prognostic potential of a tau radiotracer. A tau radiotracer could be used to determine treatment efficacy and eventually monitor treatment once clinically available. This study aimed to determine whether [18F]AV-1451 is an appropriate PET radiotracer for imaging pathological tau in PSP and could differentiate PSP from PD.

Material and methods

Participants and design

A total of 22 participants were recruited for this PET imaging study; 6 patients with a diagnosis of PSP were compared to 6 patients with PD and 10 healthy controls (HC). All PSP patients met the National Institute for Neurological Disorder and Society criteria for probable PSP. The PSP Rating Scale (PSPRS) was used to assess disease severity in PSP patients.[27] PD diagnoses were confirmed using the UK Parkinson's Disease Society Brain Bank Criteria. Both PSP and PD underwent the Unified Parkinson's Disease Rating Scale Part III (UPDRS-III) to assess motor symptom severity.[28] The Montreal Cognitive Assessment (MoCA) and Beck Depression Inventory II (BDI) were used to assess participants' general cognitive capabilities and depression levels, respectively. Exclusion criteria for all participants were as follows: no other history of neurodegenerative disorder(s), no alcohol or drug dependency/abuse, unable or unwilling to undergo PET and/or magnetic resonance imaging (MRI) scan. Additionally, control participants must not have had any history of neurological or psychiatric disorders. Written informed consent was obtained from all participants. This study was approved by the Research Ethics Board at the Centre for Addiction and Mental Health, University of Toronto and abided by the ethical guidelines of the Toronto Academic Health Science Network.

Radiosynthesis of [18F]AV-1451

The method of Shoup et al. was followed with some deviations. The radiosynthesis was carried out using a commercial radiosynthesis module (Synthra RNplus). [18F]Fluoride was produced by the $^{18}O(p,n)^{18}F$ nuclear reaction using >95% enriched [18O]H$_2$O. The aqueous [18F]fluoride was trapped on a Chromafix ion-exchange

30-PS-HCO₃ resin, and eluted into a glassy carbon reactor with 1 mL of a solution containing 1.36 mg of potassium carbonate (K_2CO_3) and 4,7,13,16,21,24-hexaoxa-1,10-diazabicyclo[8.8.8.]hexacosane (Kryptofix® 222, 13–15 mg) in 90% aqueous methanol. The solution was dried by a combination of heat (90°C), vacuum, and N_2 flow (350 mL/min) for 5 min. After cooling the reactor to 60°C, a solution of precursor (tert-butyl 7-(6-nitropyridin-3-yl)-5H-pyrido[4,3-b]indole-5-carboxylate, 0.5 mg) in anhydrous dimethylsulphoxide (0.7 mL) was added, stirred, and heated at 130°C for 7 min. Upon cooling to <40°C, a 2% solution of trifluoroacetic acid (3.7 mL) was added, and the reaction mixture was purified by HPLC using a Phenomenex Gemini NX C18, 5μ, 250 × 10 mm column, flow 6 mL/min using 50% methanol: 50% $H_2O + 0.2\%$ TFA. The desired fraction containing [¹⁸F]T807 was collected, diluted with 25 mL of USP grade water and 2 mL of USP grade 1 N sodium bicarbonate, and trapped on a pre-conditioned reverse-phase cartridge (Waters Sep-Pak tC18+). After washing the cartridge with USP grade water (5 mL) to remove salts and residual methanol, the radiotracer was eluted with USP ethanol (1 mL), chased with USP saline (10 mL), then passed through a sterile 0.2μ filter into a sterile, pyrogen-free dose vial. Radiochemical yields were 40%–60% (uncorrected for decay) in a synthesis time of 50–55 min with radiochemical purities of >99.5% and specific activities of 240–560 GBq/μmole at end-of-synthesis.[29]

PET imaging

PET scans were acquired on a high-resolution PET/CT Siemens-Biograph HiRez XVI (Siemens Molecular Imaging Knoxville, TN, USA). Prior to the PET scan, a low-dose (0.2 mSv) CT scan was performed and used for attenuation correction. In order to prevent head movement during the PET scan, a thermoplastic facemask was custom-fitted to each participant and attached to a head-fixation system (Tru-Scan Imaging, Annapolis). A bolus of [¹⁸F]AV-1451 was injected into the antecubital vein via an intravenous line, and a 90-min PET scan was acquired. Emission list mode data were then rebinned into a series of 3D sinograms that were corrected for attenuation and scatter. The PET acquisition from 0 to 90 min was binned into 28 frames (8 × 15s, 3 × 60s, 5 × 120s, 5 × 300s, 5 × 600s). Fourier rebinning was then applied to convert the 3D sinograms to 2D sinograms. 2D filter back projection was used to reconstruct the 2D sinograms into image space. Images were reconstructed with a spatial resolution of 2 × 2 × 2 mm ($x \times y \times z$).

A 3.0 T GE Discovery MR750 MRI system (General Electric, Milwaukee, WI) was used to acquire whole-brain 2D proton density-weighted (84 slices; 2.0 mm slice thickness) and T1-weighted (200 slices; 0.9 mm slice thickness) MRI scans. Proton density-weighted MRIs were obtained to provide anatomical reference for region of interest (ROI) delineation of the PET scans. T1-weighted MRIs were used for spatial normalization of parametric PET images.

Image analysis

Standardized uptake value ratios (SUVRs) were calculated in reference to the cerebellar cortex, a region considered free of pathological tau in PSP, for each ROI.[33] ROIs were delineated using Region of Mental Interest (ROMI) software, an automated program designed by Rusjan and colleagues (2006) based on standardized atlases.[30–32] Using Statistical Parametric Mapping software (SPM8, Welcome Department of Imaging Neuroscience, London, UK), each individual's MRI (GE 3 T, proton density weighted, 1 mm slice thickness) was used to non-linearly transform a standardized brain template (International Consortium for Brain Mapping/Montreal Neurological Institute 152 MRI) with predefined cortical and subcortical ROIs. The individual ROI template was then further refined using SPM8 based on gray matter probability of the segmented MRI. The refined individual ROIs were aligned and resliced using a normalized mutual information algorithm to match the individual's PET scan. Time-activity curves (TACs) were then extracted for each ROI.

ROIs used for analysis were chosen based on brain regions implicated with tau pathology in PSP postmortem studies, these included the frontal lobe, parietal lobe, ventral striatum, caudate, putamen, globus pallidus, thalamus, and dentate nucleus.[33] The ROI template used in ROMI did not contain the dentate nucleus; therefore, this ROI was drawn manually, and TACs were extracted using MarsBaR tool box.[34] Standardized uptake values (SUVs) for each ROI were calculated using the TAC values. SUV over time in a target region is based on the relationship between the concentration of radioactivity in the region (C_{img}, kBq/mL), the injected dose into the subject (ID, MBq), and the subject's body weight (BW, kg)

$$SUV(t) = \frac{C_{PET}(t)}{ID/BW} \tag{1}$$

SUVR values were averaged from 60 to 90 min post-injection. Rousset et al.[35] partial volume correction (PVC) was performed in order to control for differences in radiotracer uptake due to atrophy in the patient groups.

Statistical analysis

[^{18}F]AV-1451 SUV and SUVR were compared across groups using an independent samples analysis of variance (ANOVA) and Bonferroni post hoc testing in IMB SPSS Statistics 20 to test significant differences in [^{18}F]AV-1451 uptake between PSP, PD, and HC. Pearson correlation was used to test whether [^{18}F]AV-1451 uptake was associated with age, MoCA, or UPDRS scores. Demographic factors were also analyzed to test for differences between groups. An ANOVA and Bonferroni post hoc testing were performed on age, MoCA scores, and BDI across all three participant groups. An independent samples *t*-test was performed on disease duration and UPDRS to test for differences between the PD and PSP patient groups. To test for differences in gender proportions between groups, a chi squared analysis was performed. A threshold of $p < 0.05$ was implemented to determine significance.

Results

Participant demographics

Participant demographics are shown in Table 1. There were 6 PSP patients, 6 PD patients, and 10 HC participants enrolled in this study. Although PSP patients were, on average, older than PD and HC participants, there were no significant differences in age between groups. Gender ratio across all three groups also did not differ significantly. As expected, the mean MoCA scores of PSP patients were significantly lower than the mean MoCA scores of PD patients ($t = 3.84$, $p < 0.001$) and HC ($t = 4.13$, $p < 0.001$). All PSP MoCA scores were below 26, indicating a certain level of cognitive decline. These results are consistent with the previously reported cognitive impairment in PSP and the association of tau with dementia. The mean BDI score of the PSP group was significantly greater than that of the PD group ($t = 2.79$, < 0.05) and HC group ($t = 10.1$, $p < 0.001$). PD patients had, on average a higher BDI than HC ($t = 7.19$, $p < 0.001$). Elevated BDI scores in the patient groups were expected due to their physically and mentally debilitating disorders. The mean UPDRS-III score (motor examination) of PSP patients was significantly greater than the PD patients ($t = 10.3$, $p < 0.001$), indicating more severe motor symptoms. Disease duration of PSP patients was, on average, shorter than PD disease duration; however, this difference is not significant. These scores are consistent with the aggressive nature of the neurodegenerative process in PSP. There were no significant differences in amount of [^{18}F]AV-1451 injected across the three groups.

Standardized uptake values

SUVs were calculated from 60 to 90 min post-injection of [^{18}F]AV-1451. This time-point was based on the TACs in Figure 1 and SUVR-time graphs (supplemental Figure 2), indicating that equilibrium has been reached. Values are presented in Table 2. SUVs ranged from 1.10 to 2.13 in the PSP group, 0.944 to 2.23 in the PD group, and 0.910 to 1.99 in the HC group. In all groups, the cerebellar reference region showed the lowest SUV compared to all other ROIs. There were no significant differences when comparing ROI SUVs across the three participant groups.

Table 1. Participant demographics.

	PSP ($n = 6$)	PD ($n = 6$)	HC ($n = 10$)
Age in years	72.2 (6.77)	63.67 (9.61)	65.9 (9.93)
Gender (M/F)	2/4	3/3	2/8
MoCA score	20.8 (2.39)*,**	28.3 (0.715)	26.6 (1.51)
BDI score	14.8 (2.32)***	11.2 (2.23)**	2.56 (2.30)
UPDRS-III score	60.7 (7.58)*	26.3 (3.01)	–
PSPRS score	45.0 (9.81)	–	–
Disease duration in years	4.00 (1.41)	5.50 (2.43)	–
Amount injected in mCi	4.86 (0.263)	4.72 (0.261)	4.95 (0.458)

PSP: progressive supranuclear palsy; PD: Parkinson's disease; HC: healthy controls; MoCA: Montreal Cognitive Assessment; BDI: Beck Depression Inventory II; PSPRS: Progressive Supranuclear Palsy Rating Scale; UPDRS-III: Unified Parkinson's Disease Rating Scale Part III. Mean values ($\pm$ standard deviation).
*Significantly different from PD at $p < 0.001$.
**Significantly different from HC at $p < 0.001$.
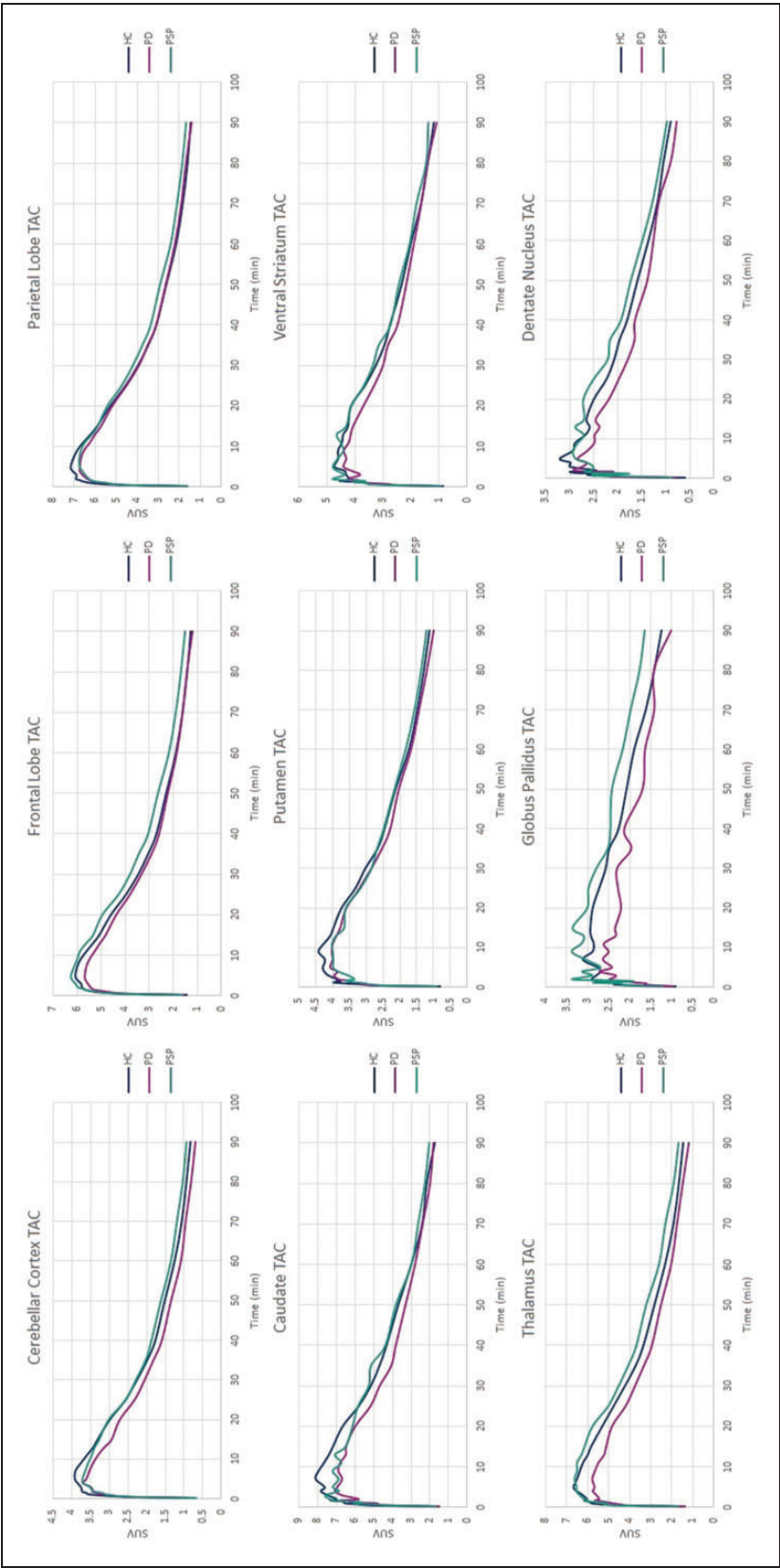***Significantly different from PD at $p < 0.05$.

Figure 1. Group mean time-activity curves (TACs) of each ROI.
PSP: progressive supranuclear palsy; PD: Parkinson's disease; HC: healthy controls.

Standardized uptake value ratios

Mean SUVR values (60–90 min) were calculated using the cerebellar cortex as a reference region. Parametric images (Figure 2) were created for each group to

Table 2. Standardized uptake values.

ROI	PSP	PD	HC
Frontal lobe	1.66 (0.360)	1.57 (0.566)	1.40 (0.352)
Parietal lobe	1.85 (0.445)	1.88 (0.664)	1.61 (0.405)
Ventral striatum	1.51 (0.397)	1.54 (0.791)	1.30 (0.360)
Caudate	2.13 (0.547)	2.23 (0.830)	1.99 (0.711)
Putamen	1.33 (0.425)	1.35 (0.498)	1.23 (0.367)
Globus pallidus	1.74 (0.658)	1.41 (0.528)	1.33 (0.400)
Thalamus	1.93 (0.641)	1.65 (0.663)	1.58 (0.405)
Dentate nucleus	1.19 (0.113)	1.21 (0.122)	1.22 (0.180)
Cerebellar cortex	1.01 (0.325)	0.944 (0.330)	0.910 (0.243)

PSP: progressive supranuclear palsy; PD: Parkinson's disease; HC: healthy controls; ROI: region of interest. Mean values (± standard deviation) from 60 to 90 min.

visually depict the uptake in PSP, PD, and HC using SUVR. PVC parametric images and the corresponding non-corrected images are depicted in supplemental Figure 1. The subcortical regions, primarily the striatal area, had the strongest signals across all three groups. In PSP, there was a notable amount of atrophy. This atrophy was confirmed by visual inspection of the individual MRIs. PVC was performed to address the possible effect of frontal atrophy and ventricular enlargement on the uptake in PSP patients.

ROI analysis of SUVRs across groups is presented in Table 3 and Figure 3. SUVRs for PSP ranged from 1.19 to 2.17 (dentate nucleus and caudate, respectively). The caudate, thalamus, and parietal lobe had the greatest SUVRs in PSP. SUVRs for PD ranged from 1.21 (dentate nucleus) to 2.39 (caudate). The caudate and putamen presented with the highest SUVRs. Regions with the lowest SUVR in PD included the frontal lobe, inferior parietal lobe. The dentate nucleus had the lowest SUVR in the HC group. The highest SUVR in HC was the caudate, followed by the parietal lobe and
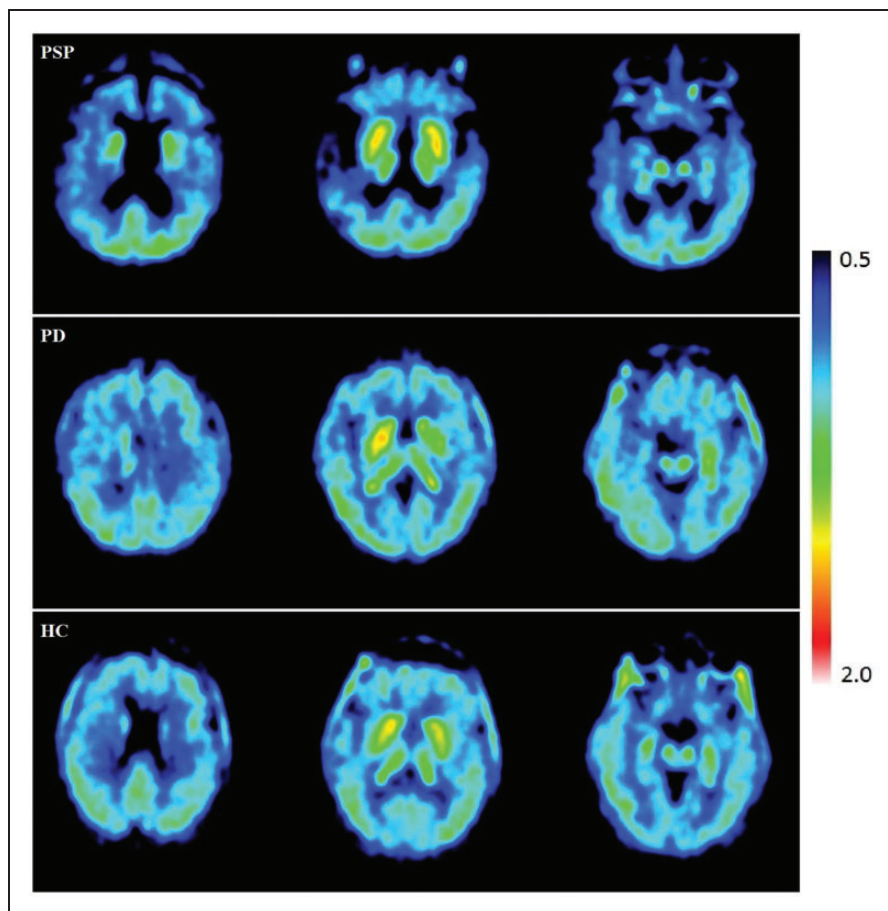

Figure 2. Individual parametric images of SUVR 60–90 min corrected for partial volume effects.
PSP: progressive supranuclear palsy; PD: Parkinson's disease; HC: healthy controls.

Table 3. Standardized uptake value ratios.

ROI	PSP	PD	HC
Frontal lobe	1.68 (0.215)	1.70 (0.232)	1.51 (0.238)
Parietal lobe	1.88 (0.236)	2.04 (0.402)	1.72 (0.240)
Ventral striatum	1.51 (0.239)	1.57 (0.342)	1.42 (0.129)
Caudate	2.17 (0.590)	2.39 (0.301)	2.13 (0.583)
Putamen	1.31 (0.215)	1.43 (0.0723)	1.37 (0.243)
Globus pallidus	1.71 (0.203)	1.57 (0.484)	1.47 (0.278)
Thalamus	1.91 (0.219)	1.72 (0.191)	1.70 (0.153)
[a]Dentate nucleus	1.19 (0.113)	1.21 (0.122)	1.22 (0.180)

PSP: progressive supranuclear palsy; PD: Parkinson's disease; HC: healthy controls; ROI: region of interest. Partial volume corrected mean values ($\pm$ standard deviation) from 60 to 90 min using the cerebellar cortex as a reference region.
[a]Dentate nucleus is not partial volume corrected due to manual delineation.

the thalamus. All ROIs had SUVRs greater than 1, indicating uptake of [^{18}F]AV-1451 greater than that of the cerebellar reference region.

There were no ROIs that had a significantly higher SUVR in PSP patients compared to PD and HC. PSP SUVRs were elevated (not significantly) compared to HC in the frontal lobe, parietal lobe, ventral striatum, caudate, globus pallidus, and the thalamus.

Clinical correlations

Due to the cognitive component that accompanies many tauopathies, MoCA scores were tested against [^{18}F]AV-1451 uptake across all participants. Pearson correlation results indicated that MoCA scores were not predictors of SUVRs in any of the ROIs analyzed, using the cerebellar cortex as a reference region.

The final correlation tested was between [^{18}F]AV-1451 uptake and PSPRS and UPDRS scores, with the question whether severity of motor symptoms severity could be associated with a greater tau burden. However, there was no correlation between either of the rating scales for motor symptoms scores and [^{18}F]AV-1451 uptake.

Discussion

This study was designed to contribute to the expanding research of tau in vivo imaging. While tau is involved in many neurodegenerative disorders, PSP is one that has been underrepresented in many tau neuroimaging studies. In order to advance the current knowledge regarding tau imaging and PSP, we investigated the PET radiotracer [^{18}F]AV-1451 in this patient population. It was predicted that [^{18}F]AV-1451 uptake in cortical and subcortical regions would be

significantly greater in PSP patients compared to PD patients and HC.

Using SUVR to measure [^{18}F]AV-1451 uptake in the brains of PSP, PD, and HC participants revealed some changes in a few ROIs, though not the differences that were expected. SUVR was not significantly higher in PSP compared to PD and HC in any of the ROIs analyzed. These results are consistent with the findings of recent post-mortem studies that indicate no significant binding of [^{18}F]AV-1451 to PSP brain slices.[23,24]

Inspection of individual MRIs revealed considerable enlargement of the ventricles and atrophy of the frontal lobes of PSP patients compared to PD and HC MRIs. This finding is consistent with previous MRI studies involving PSP.[36,37] Atrophy can reduce the size of ROIs, making it difficult to segment (the gray matter, white matter, and CSF) and normalize the MRI, thereby risking the possibility of inaccurate ROI delineation. Successful segmentation and normalization was achieved for all participants, and the ROI template was carefully matched to each individual PET scan. Another concern with smaller ROIs due to atrophy is the partial volume effect. This phenomenon causes "spill in" and/or "spill out" of measured radioactivity in any given ROI. "Spill out" is of particular interest in the cases of small ROIs with high activity because the measured activity within the ROI "spills out" into neighboring areas, making the small ROI appears to have less retention of the radiotracer than is in fact true. Due to the amount of atrophy that was seen on the MRIs in the PSP patients, we believed that PVC should be applied in order to control for the potential "spill out" effect.

Partial volume effect correction was performed on all PET scans, regardless of the participant group, to ensure objectivity and consistency between the three groups and also within groups. As expected, partial volume effect correction increased the SUVRs of some PSP ROIs. However, this correction also increased the SUVRs of the same ROIs in PD and HC; therefore, there were still no significant increases in PSP SUVR compared to PD and HC.

Tauopathies differ from each other in many ways: symptomology, tau load pattern, etc. The ability of an imaging agent to bind all conformations of tau is a critical characteristic for successful imaging of tau in vivo in all tauopathies. Tauopathies contain varying ratios of tau isoforms. The ratio in AD is similar to that of a healthy brain with an equal 3R to 4R ratio, as indicated by its major tau bands of 60, 64, and 68 kDa and minor band of 72 kDa.[10] PSP and CBD tau aggregates run as major bands of 64 and 68 kDa and minor band at 72 kDa and are primarily composed of 4R isoforms, while Pick bodies in Pick's disease (PiD) are generally formed by 3R isoforms, as
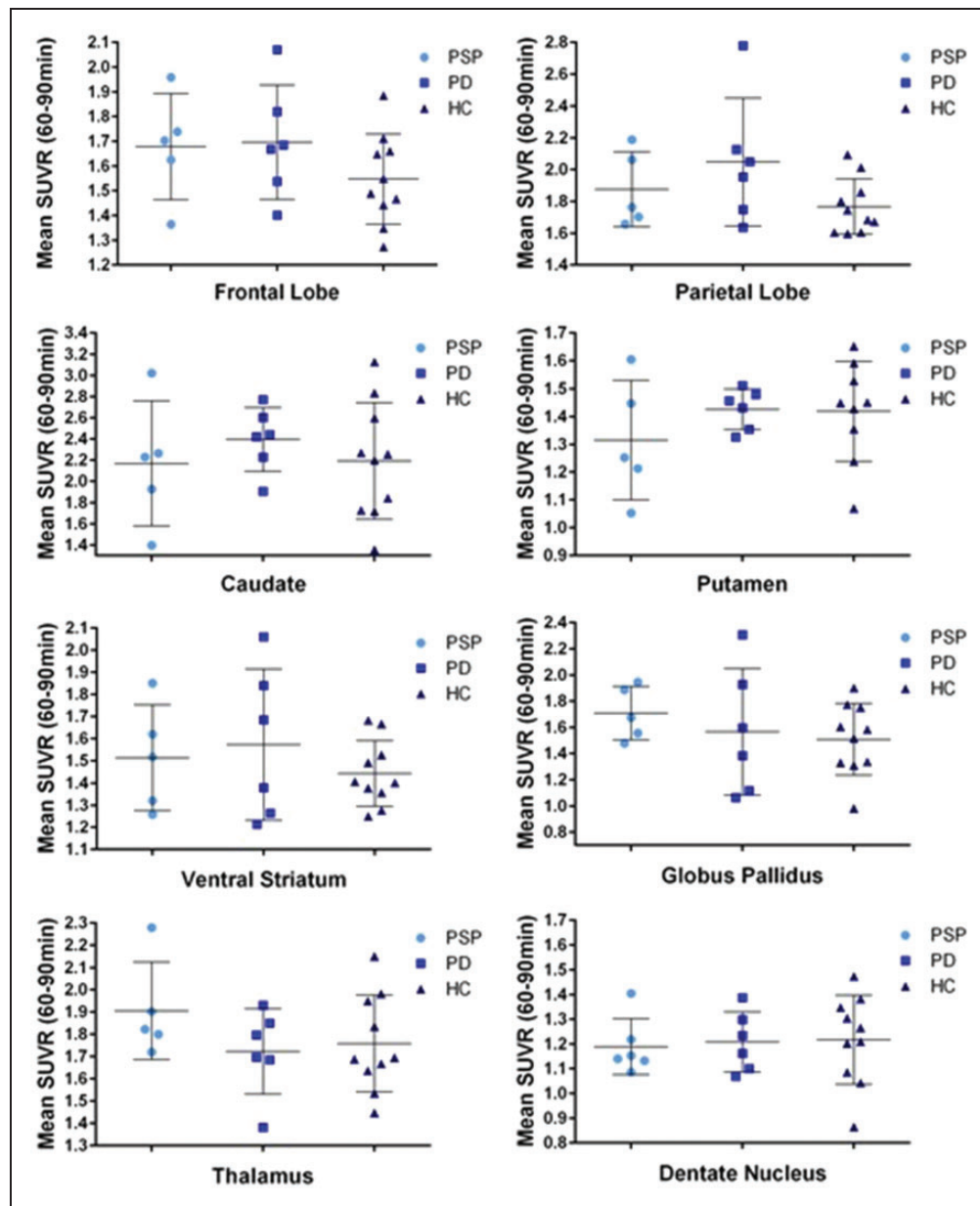
Figure 3. Group mean SUVR 60–90 min values by group.
PSP: progressive supranuclear palsy; PD: Parkinson's disease; HC: healthy controls; SUVR: standardized uptake value ratio.

demonstrated by the major tau bands of 60 and 64 kDa and a minor band of 68 kDa. An ideal radiotracer for all tauopathies would be capable of imaging both isoforms. Previous in vitro and in vivo work with [18F]AV-1451 on AD brain slices and AD patients suggests that this radioligand is capable of binding both 3 R and 4 R tau isoforms.[22,25,26] Additionally, when tested in post-mortem tissue, [18F]AV-1451 phosphor screen autoradiography demonstrated signal in AD but no signal in PSP and CBD (4R), and PiD (3R). Therefore, [18F]AV-1451 does not seem to preferentially image one tau isoform over the other. Lack of

signal in PSP brain slices and the absence of differences between our groups are not likely due to the 4 R tau isoform present in PSP tau inclusions.

Another important difference between AD and other tauopathies is the structure of its tau aggregates. AD tau inclusions form primarily PHF conformations, with only approximately 5% of total tau load represented by straight filaments.[38] PHFs have a diameter of approximately 8–20 nm and periodicity of 80 nm. PSP and other tauopathies (CBD and PiD) present primarily with straight filaments and to a much lesser degree of PHFs.[10]

The findings of this study, and the earlier post-mortem autoradiographic studies suggest that [18F]AV-1451 may not be appropriate for imaging pathological tau in PSP.[23,24] [18F]AV-1451 was initially screened for tau inclusions in PHF conformations from AD brains; therefore, the hits that were produced from these screenings were compounds that bound PHF tau and not necessarily straight filaments of tau. The first testing in vitro performed on AD brains slices and in vivo testing on MCI, and AD patients indicated that [18F]AV-1451 could bind PHF tau and differentiate AD from MCI and HC, thereby initially designating [18F]AV-1451 as a promising radiotracer for imaging tau in vivo.[22,25] Further studies also demonstrated that [18F]AV-1451 was capable of binding tau in AD.[23,26] However, when [18F]AV-1451 is applied to PSP cases, this current clinical research supports the previously published post-mortem data indicating that [18F]AV-1451 does not bind pathological tau in PSP.[23] The most probable reason could be that [18F]AV-1451 selectively binds PHF tau but not straight filaments of tau.

In order to effectively image all tauopathies, multiple PET radiotracers may need to be developed. Specificity from certain isoforms and conformations of pathological tau could prohibit one single radiotracer from being an appropriate measure of tau pathology in the brain. Further investigation into radiotracers targeting straight filaments of tau, as well as the 3 R and 4 R isoform should be performed.

For this pilot study, we decided to analyze the uptake of [18F]AV-1451 using SUVR, a semi-quantitative and less invasive method. A full in vivo pharmacokinetic analysis of [18F]AV-1451 has recently been published by Wooten et al.[39] Participants included controls, subjects with a history of traumatic brain injury, and mild cognitive impairment. The total volume of distribution (V_T) was calculated using a two-tissue reversible compartmental model with plasma input function, as this demonstrated the best fit. Static SUVR from 80 to 100 min, using the cerebellum as a reference region, was found to have a high correlation with the well-fit two-tissue compartment model results. Therefore, this suggests that SUVR is an appropriate measure of uptake of [18F]AV-1451.[39]

Conclusion

The aim of this study was to determine whether [18F]AV-1451 is an appropriate radiotracer for imaging pathological tau in PSP patients. Retention of [18F]AV-1451 was not significantly higher in PSP compared to PD and HC in any of the ROIs analyzed in this study. We also tested whether general cognition could predict the uptake of [18F]AV-1451 because of the relationship between tau deposition and cognitive decline. There was no significant relationship between MoCA scores and [18F]AV-1451 SUVR in any of the ROIs. There was also no correlation with [18F]AV-1451 and age, PSPRS, or UPDRS. Based on our preliminary findings and previous literature regarding the different conformations of tau pathology found in AD and PSP, [18F]AV-1451 may only bind to PHF tau and not the straight filaments of tau found in PSP. If this is the case, then [18F]AV-1451 is not a valid tau radiotracer for PSP and other radiotracers should be investigated.

Declaration of conflicting interests

The author(s) declared no potential conflicts of interest with respect to the research, authorship, and/or publication of this article.

Authors' contributions

SC: acquisition of data, analysis and interpretation of data, draft manuscript for intellectual content

SSC: analysis and interpretation of data, critical revision of manuscript for intellectual content

YK: acquisition of data, critical revision of manuscript for intellectual content

PR: analysis and interpretation of data, critical revision of manuscript for intellectual content

MH: critical revision of manuscript for intellectual content

CG: critical revision of manuscript for intellectual content

JK: critical revision of manuscript for intellectual content

AEL: study concept and design, critical revision of manuscript for intellectual content

AW: acquisition of data, critical revision of manuscript for intellectual content

SH: study concept and design, critical revision of manuscript for intellectual content, study supervision

APS: study concept and design, critical revision of manuscript for intellectual content, study supervision.

Supplementary material

Non-PVC images and group mean SUVR-time graphs are available in the supplementary section. Supplementary material for this paper can be found at http://journals.sagepub.com/doi/suppl/10.1177/0271678X16683695.

References

1. Golbe L. The tau of PSP: a long road to treatment. *Mov Disord* 2014; 29: 431–434.
2. Liscic RM, Srulijes K, Gröger A, et al. Differentiation of progressive supranuclear palsy: clinical, imaging and laboratory tools. *Acta Neurol Scand* 2013; 127: 362–370.
3. Litvan I, Agid Y, Calne D, et al. Clinical research criteria for the diagnosis of progressive supranuclear palsy (Steele-Richardson-Olszewski syndrome): report of the NINDS-SPSP international workshop. *Neurology* 1996; 47: 1–9.
4. Golbe LI. Progressive supranuclear palsy. *Semin Neurol* 2014; 34: 151–159.
5. Kobylecki C, Jones M, Thompson J, et al. Cogntive-behavioural features of progressive supranuclear palsy syndrome overlap with frontotemporal dementia. *J Neurol* 2015; 262: 916–922.
6. Osaki Y, Ben-Shlomo Y, Lees AJ, et al. Accuracy of clinical diagnosis of progressive supranuclear palsy. *Mov Disord* 2004; 19: 181–189.
7. Lees AJ, Hardy J and Revesz T. Parkinson's disease. *Lancet* 2009; 373: 2055–2066.
8. Dickson DW. Neuropathologic differentiation of progressive supranuclear palsy and corticobasal degeneration. *J Neurol* 1999; 246: II6–II15.
9. Avila J, Lucas JJ, Perez M, et al. Role of tau protein in both physiological and pathological conditions. *Physiol Rev* 2004; 84: 361–384.
10. Spillantini MG and Goedert M. Tau pathology and neurodegeneration. *Lancet Neurol* 2013; 12: 609–622.
11. Iqbal K, Liu F, Gong C-X, et al. Tau in Alzheimer disease and related tauopathies. *Curr Alzheimer Res* 2010; 7: 656–664.
12. Shahani N and Brandt R. Functions and malfunctions of the tau proteins. *Cell Mol Life Sci* 2002; 59: 1668–1680.
13. Avila J and Lucas J. Role of tau protein in both physiological and pathological conditions. *Physiol Rev* 2004; 34: 361–384.
14. Noble W, Hanger DP, Miller CCJ, et al. The importance of tau phosphorylation for neurodegenerative diseases. *Front Neurol* 2013; 4: 88.
15. Thal DR, Attems J and Ewers M. Spreading of amyloid, tau, and microvascular pathology in Alzheimer's disease: findings from neuropathological and neuroimaging studies. *J Alzheimer's Dis* 2014; 42: 421–429.
16. Grijalvo-Perez A and Litvan I. Corticobasal degeneration. *Semin Neurol* 2014; 34: 160–173.
17. Kepe V, Bordelon Y, Boxer A, et al. PET imaging of neuropathology in tauopathies: progressive supranuclear palsy. *J Alzheimers Dis* 2013; 36: 145–153.
18. Okamura N, Furumoto S, Harada R, et al. Novel 18F-labeled arylquinoline derivatives for noninvasive imaging of tau pathology in Alzheimer disease. *J Nucl Med* 2013; 54: 1420–1427.
19. Okamura N, Furumoto S, Fodero-Tavoletti MT, et al. Non-invasive assessment of Alzheimer's disease neurofibrillary pathology using 18F-THK5105 PET. *Brain* 2014; 137: 1762–1771.
20. Okamura N, Furumoto S, Harada R, et al. In vivo selective imaging of tau pathology in Alzheimer's disease with 18F-THK5117. *J Nucl Med* 2014; 55: 18–19.
21. Maruyama M, Shimada H, Suhara T, et al. Imaging of tau pathology in a tauopathy mouse model and in Alzheimer patients compared to normal controls. *Neuron* 2013; 79: 1094–1108.
22. Xia CF, Arteaga J, Chen G, et al. [(18)F]T807, a novel tau positron emission tomography imaging agent for Alzheimer's disease. *Alzheimers Dement* 2013; 9: 666–676.
23. Marquie M, Normandin MD, Vanderburg CR, et al. Validating novel tau positron emission tomography tracer [F-18]-AV-1451 (T807) on postmortem brain tissue. *Ann Neurol* 2015; 78: 787–800.
24. Sander K, Lashley T, Gami P, et al. Characterization of tau positron emission tomography tracer [18F] AV-1451 binding to postmortem tissue in Alzheimer's disease, primary tauopathies, and other dementias. *Alzheimers Dement* 2016; 12: 1116–1124.
25. Chien DT, Bahri S, Szardenings AK, et al. Early clinical PET imaging results with the novel PHF-tau radioligand [F-18]-T807. *J Alzheimers Dis* 2013; 34: 457–468.
26. Schwarz AJ, Yu P, Miller BB, et al. Regional profiles of the candidate tau PET ligand 18F-AV-1451 recapitulate key features of Braak histopathological stages. *Brain* 2016; 139: 1539–1500.
27. Golbe L and Ohman-Strickland PA. A clinical rating scale for progressive supranuclear palsy. *Brain* 2007; 130: 1552–1565.
28. Goetz CG, Tilley BC, Shaftman SR, et al. Movement Disorder Society-Sponsored Revision of the Unified Parkinson's Disease Rating Scale (MDS-UPDRS): scale presentation and clinimetric testing results. *Mov Disord* 2008; 23: 2129–2170.
29. Shoup TM, Yokell DL, Rice PA, et al. A concise radiosynthesis of the tau radiopharmaceutical, [18F]T807. *J Label Compd Radiopharm* 2013; 56: 736–740.
30. Talairach J and Tournoux P. *Co-planar stereotaxic atlas of the human brain. 3-dimensioanl proportional system: an approach to cerebral imaging.* New York: Thieme Medical Publishers, 1988.
31. Kabani N, Collins D and Evans A. A 3d neuroanatomical atlas. In: *4th international conference on functional mapping of the human brain*, Montreal, Quebec, Canada, 7–12 June 1988, pp.7–12. Montreal: Organization for Human Brain Mapping.
32. Rusjan P, Mamo D, Ginovart N, et al. An automated method for the extraction of regional data from PET images. *Psychiatry Res* 2006; 147: 79–89.
33. Williams DR, Holton JL, Strand C, et al. Pathological tau burden and distribution distinguishes progressive supranuclear palsy-parkinsonism from Richardson's syndrome. *Brain* 2007; 130: 1566–1576.

34. Brett M, Anton JL, Valabregue R, et al. Region of interest analysis using the MarsBar toolbox for SPM 99. *Neuroimage* 2002; 16: S497.
35. Rousset OG, Ma Y and Evans AC. Correction for partial volume effects in PET: principle and validation. *J Nucl Med* 1998; 39: 904–911.
36. Giordano A, Tessitore A, Corbo D, et al. Clinical and cognitive correlations of regional gray matter atrophy in progressive supranuclear palsy. *Park Relat Disord* 2013; 19: 590–594.
37. Massey LA, Micallef C, Paviour DC, et al. Conventional magnetic resonance imaging in confirmed progressive supranuclear palsy and multiple system atrophy. *Mov Disord* 2012; 27: 1754–1762.
38. Spillantini MG, Bird TD and Ghetti B. Frontotemporal dementia and Parkinsonism linked to chromosome 17: a new group of tauopathies. *Brain Pathol* 1998; 8: 387–402.
39. Wooten D, Guehl N, Verwer E, et al. Pharmacokinetic evaluation of the tau PET radiotracer [^{18}F]T807 ([^{18}F]AV-1451) in human subjects. *J Nucl Med* 2016; 807: 1–27.